Dalton Transactions

ROYAL SOCIETY OF CHEMISTRY

PAPER

View Article Online
View Journal | View Issue

Cite this: *Dalton Trans.*, 2023, **52**, 11158

Co-generation of palladium nanoparticles and phosphate supported on metal–organic frameworks as hydrogenation catalysts†

Yohei Takashima, * Seiko Tetsusashi, Mai Takano, Shintaro Tanaka, Yui Murakami, Takaaki Tsuruoka and Kensuke Akamatsu*

Received 23rd December 2022,
Accepted 10th July 2023

DOI: 10.1039/d2dt04109j

rsc.li/dalton

In this study, we demonstrated the direct synthesis of sodium dihydrogen phosphate (PA) containing palladium nanoparticles (PdNPs) supported on a metal–organic framework (MOF). The resulting composite containing PA molecules coexisting with PdNPs demonstrated improved hydrogenation catalytic performance compared to the composites without PA.

Introduction

Hydrogenation reactions are crucial not only for the bulk chemicals industry but also for synthesising fine chemicals, which require the use of catalysts. Among the catalysts used for hydrogenation reactions, PdNPs are most common because they exhibit a high catalytic activity that the surrounding reaction environment can tune.[1] PdNPs can be supported on various substrates such as metal oxides,[2] organic polymers,[3] and porous materials. Recently, metal–organic frameworks (MOFs) have been investigated as substrates for PdNP immobilisation.[4–7]

MOFs are novel porous crystalline materials composed of metal ions and organic linkers. MOFs exhibit advantages compared to other conventional porous materials. The porous structure of MOFs can be tuned precisely by selecting the metal-ion component and the organic linker to interact strongly with guest molecules.[8–14] The applications of gas molecules as guest particles inside the MOFs pores are typically related to gas storage and separation. However, larger guest particles such as metal nanoparticles, organic dyes, and functional polymers have also been trapped inside the MOF pores to generate hybrid functional materials.[15–27] In the case of hybridisation with metal nanoparticles, the resulting materials are typically applied as catalysts because these nanoparticles lead to high catalytic activity.

Herein, hybridised MOFs with PdNPs and PA coexisting in the porous support were prepared and evaluated as catalysts for the hydrogenation of olefin substrates. Phosphate particles exhibit strong interaction with olefin substrates, which may have a positive effect on hydrogenation reactions through PdNPs in the fabricated composites.[28] MOF composites modified with PdNPs and other guest molecules to control their catalytic activity have been previously reported. However, the modified MOF porous structures were obtained following a stepwise approach.[29,30] The proposed system comprises PdNPs and PA molecules that were co-generated inside the MOF pores to obtain a more homogeneous immobilisation of the particles in the pores to enhance their catalytic activity.

Experimental

General methods

All reagents unless otherwise stated were obtained from commercial sources and were used without further purification. X-ray powder diffraction data were collected on a Rigaku RINT-2200 Right System (Ultima IV) diffractometer with CuKα radiation. Thermogravimetric analyses were recorded on a Rigaku Thermo plus TG-8120 apparatus in the temperature range between 298 and 773 K at a heating rate of 5 K min^{-1}. The TEM observations were performed with a JEOL JEM-1400 transmission electron microscopy (TEM) system operating at 120 kV. ICP analyses were conducted by ICP AES (SPS 7800, Seiko Instruments). ^{1}H NMR spectra were recorded on a JEOL JNM-A500 spectrometer. The ^{1}HNMR chemical shifts are referenced to the residual internal benzene-d6. FT-IR spectra were obtained using a Spectrum Two spectrometer (PerkinElmer) using ATR technique. Sorption isotherm measurements were recorded using an automatic volumetric adsorption apparatus (autosorb iQ, Quantachrome). Samples were evacuated under high vacuum ($<10^{-2}$ Pa) at 393 K for 2 h to remove guest molecules. XPS spectra were collected by X-ray photoelectron spectrometer (JEOL JPS-9010MC) with Mg Kα radiation. MOF

Department of Nanobiochemistry, Frontiers of Innovative Research in Science and Technolgoy (FIRST), Konan University, 7-1-20 Minatojimaminamimachi, Chuo-ku, Kobe 650-0047, Japan. E-mail: takashim@konan-u.ac.jp, akamatsu@konan-u.ac.jp

† Electronic supplementary information (ESI) available. See DOI: https://doi.org/10.1039/d2dt04109j

powders were placed on carbon substrate, and Pd 3d peaks were observed.

Synthesis of MIL-101

Chromium(III) nitrate (4.00 g, 10.0 mmol), benzene-1,4-dicarboxylic acid (1.64 g, 10.0 mmol) and HNO_3 (10.0 mmol) were dispersed in water (50 mL). The mixture was transferred to Teflon-lined stainless steel autoclave. The resulting suspension was heated at 220 °C for 8 h under hydrothermal condition. The reaction product was finally obtained after washing three times with DMF under sonication.

$Pd(OAc)_2$ accommodation in MIL-101

To 5 ml of $Pd(OAc)_2$ acetone solutions (6 mM, 12 mM, 24 mM and 36 mM), was added 25 mg of MIL-101 and the resulting suspensions were stirred at 26 °C for 15 h. After filtration, washing with acetone under sonication and drying *in vacuo*, powder samples ($Pd(OAc)_2$@MIL-101(x) x = 12, 24, 36) were obtained.

Syntheses of PdNPs/PA@MIL-101(x, y)

To y mM (y = 30, 120 and 480) MeOH solution of $NaPH_2O_2$ (5 mL) was added 20 mg of $Pd(OAc)_2$@MIL-101(x) (x = 6, 12, 24, 36) and the resulting suspensions were stirred at 26 °C for 30 min. After filtration, washing with 30 ml of MeOH under sonication three times and drying *in vacuo*, powder samples (PdNPs/PA@MIL-101(x, y)) were obtained.

Hydrogenation reaction of olefin substrates with H_2 gas

In a typical procedure, to PdNPs/PA@MIL-101(24, 480) (Pd: 0.04 mol%), added 1 ml of 1-octene (6.4 mmol) and heated at 70 °C under H_2 (1 atm). The reaction yields of octane and 2-octene were determined as ^{1}HNMR yields using the integrals of both reactant and products.

Results and discussion

A Cr-based MIL-101 was used as the MOF using two cage-like pore diameters (2.9 and 3.4 nm) for the immobilisation of PdNPs and PAs (Fig. 1).[31–33] To generate PdNPs and PA simultaneously inside the MOF pores, the PdNP precursor was introduced by impregnation using palladium acetate ($Pd(OAc)_2$). The degassed MIL-101 was mixed with an acetone solution of $Pd(OAc)_2$ at 26 °C for 18 h to obtain $Pd(OAc)_2$@MIL-101.[34] The amount of $Pd(OAc)_2$ adsorbed inside the MOF pores was determined by inductively coupled plasma (ICP) analysis of the sample obtained after decomposing $Pd(OAc)_2$@MIL-101 using strong acids. These results indicated that the amount of Pd $(OAc)_2$ in the MIL-101 structure could be controlled through the concentration of the $Pd(OAc)_2$ solution (in acetone) during impregnation (Fig. S1†); more amount of $Pd(OAc)_2$ was accommodated by the $Pd(OAc)_2$ solution with higher concentration. Transmission electron microscopy (TEM) measurements confirmed that PdNPs were not generated in this stage of the fabrication process (Fig. S2†). Then, the resulting Pd $(OAc)_2$@MIL-101 was treated with sodium phosphinate ($NaPH_2O_2$) in MeOH to obtain PdNPs/PA@MIL-101(x, y), where x denotes the concentration of $Pd(OAc)_2$ in the acetone solution used for the impregnation process, and y denotes the concentration of the $NaPH_2O_2$ solution in MeOH. In this step, $Pd(OAc)_2$ was reduced by $NaPH_2O_2$ in PdNPs, and the $NaPH_2O_2$ was oxidised to generate PA within MIL-101.

The X-ray diffraction (XRD) and thermogravimetry (TG) results for PdNPs/PAs@MIL-101(x, 480) (x = 6, 12, 24, 36) are shown in Fig. 2A and B. From these figures, it is confirmed that the MIL-101 structures were maintained and thermally

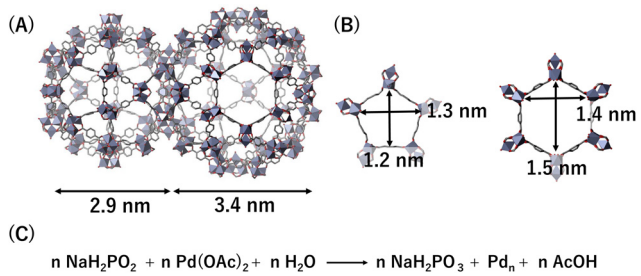

Fig. 1 Structures of (A) MIL-101 pores and (B) pore distances within clusters. (C) Proposed reaction to co-generate PdNPs and phosphate in the MOF structure.

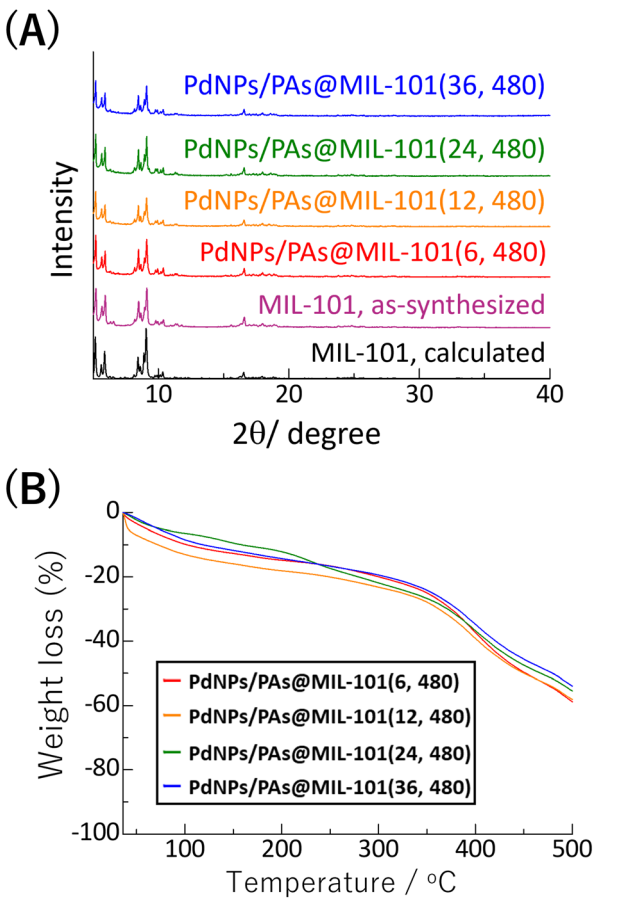

Fig. 2 (A) XRD data and (B) TG profiles of PdNPs/PAs@MIL-101(x, 480) (x = 6, 12, 24, 36).

stable up to 400 °C even after the $NaPH_2O_2$ treatment. Note that the small weight loss before 100 °C in TG profiles corresponds to the removal of H_2O molecules that were accommodated from air. Similar results are obtained in the case of PdNPs/PAs@MIL-101(x, y) (x = 6, 12, 24, 36; y = 30 and 120) (Fig. S3†). TEM images for PdNPs/PAs@MIL-101(x, 480) (x = 6, 12, 24, 36) are shown in Fig. 3A. PdNPs were homogeneously generated in all cases. Moreover, their sizes are nearly equal (Fig. 3B), indicating that $Pd(OAc)_2$ in MIL-101 is instantly reduced in excess $NaPH_2O_2$. The reduction step was followed by the rapid nucleation of PdNPs. A slightly broader size distribution obtained for PdNPs in PdNPs/PA@MIL-101(x, y) (x = 6, 12, 24, 36; y = 30 and 120) might be due to slower nucleation in less concentrated $NaPH_2O_2$ during the reduction process (Fig. S4†). The presence of PAs was confirmed by infrared radiation (IR). From the IR spectra of PdNPs/PA@MIL-101(x, y) (x = 6, 12, 24, 36; y = 30, 120, 480), the P═O stretching-vibration peaks are attributed to PA molecules (Fig. 4A and S5†). The amount of PAs in PdNPs/PA@MIL-101(x, y) (x = 6, 12, 24, 36; y = 30, 120, 480) was determined from the P (incorporated in PA) and Pd (incorporated in PdNP) ratio, using the ICP data (Fig. 4B and S6†). It should be noticed that the value of P/Pd was not equal to 1 for all samples, and it increased when the accommodated $Pd(OAc)_2$ decreased. This indicated that not all the PAs were generated by the oxidation of $NaPH_2O_2$ with $Pd(OAc)_2$. The oxidation reaction is shown in Fig. 1C. Because $NaPH_2O_2$ can react with H_2O to generate PA and hydrogen, a reaction would have also occurred to immobilise PA in the MIL-101 pores. The Pd/Cr values (determined by ICP) were almost equal before and after the $NaPH_2O_2$ treatment, which excluded the possibility that $Pd(OAc)_2$ might have been expelled from MIL-101 (Fig. S7†). In addition, we have also executed XPS measurements to elucidate the electronic state of PdNPs in PdNPs/PAs@MIL-101. The obtained Pd 3d peaks (Pd

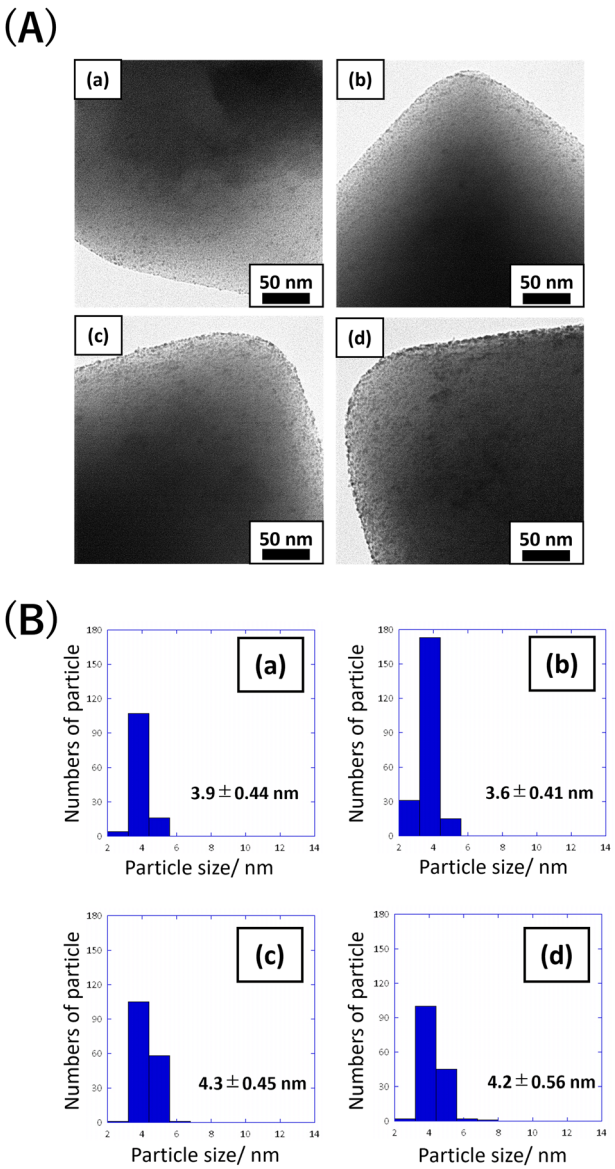

Fig. 3 (A) TEM images and (B) PdNP size distribution diagrams for PdNPs/PAs@MIL-101(x, 480): (a) x = 6, (b) x = 12, (c) x = 24, and (d) x = 36.

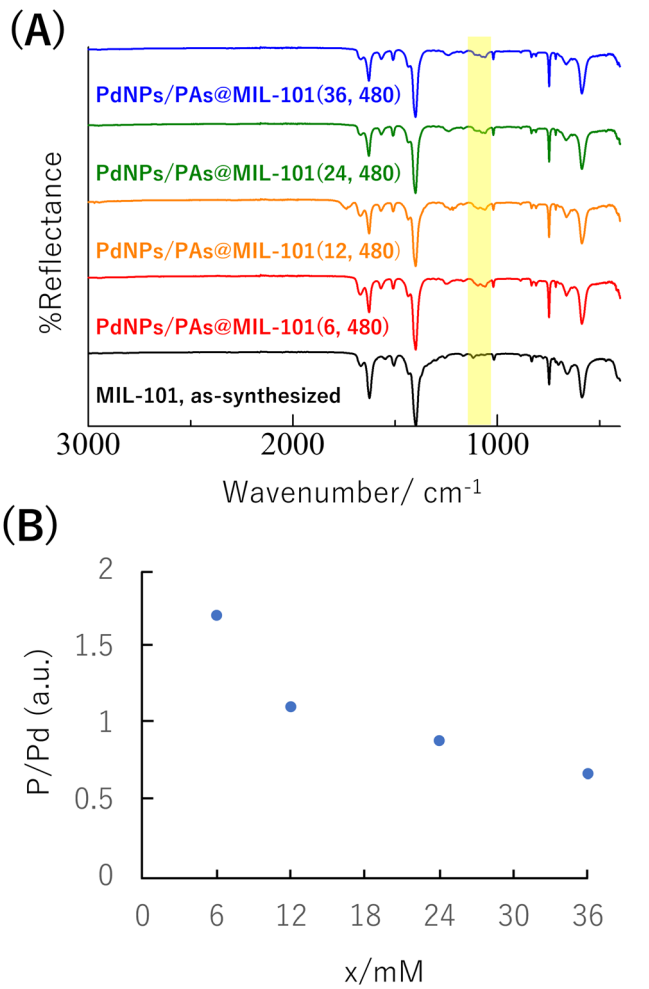

Fig. 4 (A) IR spectra of PdNPs/PAs@MIL-101(x, 480) (x = 6, 12, 24, 36). The peaks corresponding to P═O stretching vibration are highlighted in yellow. (B) P/Pd ratio in PdNPs/PAs@MIL-101(x, 480) (x = 6, 12, 24, 36).

$3d_{3/2}$ and Pd $3d_{3/5}$) could be fitted with single peak and their binding energies were 340 and 335 eV respectively, indicating that the oxidation state of PdNPs was zero; PdNPs have little interaction with PAs in MOF pores (Fig. S8†). From N_2 gas adsorption measurements at 77 K, we have also confirmed that the decrease of the porosity of MIL-101 was small even after the generations of PdNPs and PAs in the pores (Fig. S9†).

PdNPs/PAs@MIL-101(24, 480) was evaluated as the catalyst for the hydrogenation of 1-octene under H_2 gas at 1 atm. To confirm the influence of PAs in the hydrogenation reaction, the analogue catalyst without PA was synthesised (PdNPs@MIL-101) by using $Pd(OAc)_2$@MIL-101 and H_2 gas as the reductant. The reaction yields obtained with the PdNPs@MIL-101 and the PdNPs/PAs@MIL-101 (0.04 mol% Pd) catalysts are shown in Fig. 5A. It was confirmed that PAs promoted the hydrogenation reaction. The total reaction times were 3 h and 5 h for PdNPs/PAs@MIL-101 and PdNPs@MIL-101, respectively. ^{1}H NMR spectra were obtained to evaluate the evolution of the reactions. These results demonstrated that 2-octene was also generated by the isomerisation of 1-octene. Moreover, 1-octene isomerisation is more favoured with the PdNPs/PAs@MIL-101 catalyst (Fig. 5B, C, S10, and S11†). It was confirmed that PA molecules catalysed the isomerisation reaction. PdNPs/PAs@MIL-101 exhibited a higher catalytic activity towards hydrogenation than that shown by PdNPs@MIL-101, although a higher concentration of 2-octene was obtained. This product is known to exhibit lower reactivity compared to 1-octene, which indicated that PA exhibited a greater influence on the hydrogenation reaction. Although the reason for this positive effect may require further investigation, strong interaction between PA and the substrates (1-octene or 2-octene) might have positioned them closer to the PdNPs, which facilitated the subsequent hydrogenation.

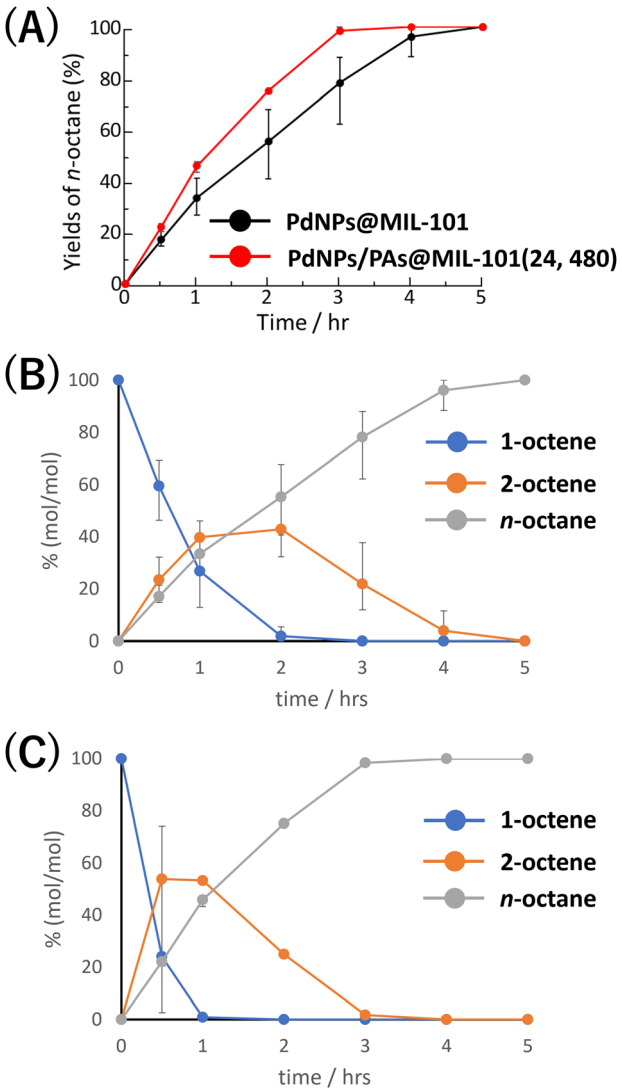

Fig. 5 (A) Evolution of the hydrogenation of 1-octene with PdNPs@MIL-101 and PdNPs/PAs@MIL-101(24, 480) catalysts. (B) 2-octene and *n*-octane yields during the hydrogenation of 1-octene with the PdNPs@MIL-101 and (C) the PdNPs/PAs@MIL-101(24, 480) catalysts.

To check the recyclability of PdNPs/PAs@MIL-101 as catalyst, we have recovered PdNPs/PAs@MIL-101 by filtration and reused. As shown in Fig. S12,† their catalytic activities were maintained without losing their structures. In addition, we have also confirmed that no reaction proceeded after the removal of PdNPs/PAs@MIL-101 by filtration, indicating that PdNPs in MIL-101 were highly stabilized not to be leaked out (Fig. S13†). The TEM image of recovered PdNPs/PAs@MIL-101 also showed the existance of PdNPs inside MIL-101 (Fig. S14†).

The hydrogenation yields with PdNPs/PAs@MIL-101 or PdNPs@MIL-101 using other alkene substrates are presented in Table 1. For linear terminal alkenes, the reaction yields were smaller as the length of their alkyl chains increased, which might be due to steric hindrance (entries 1–3). When using 1-decene as the substrate, the reaction yields were almost equal for the two catalysts, which indicated that PA molecules largely reduced the mobility of 1-decene inside the MOF pores. For the *trans*-2-octene reaction, a smaller yield than that obtained for 1-octene resulted from the intrinsic lower reactiv-

Table 1 Hydrogenation of different alkene substrates with PdNPs@MIL-101 and PdNPs/PAs@MIL-101 catalysts

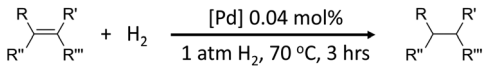

Entry	Substrate	Product	[Pd]	Yield [%]
1			PdNPs@MIL-101	78
			PdNPs/PAs@MIL-101	98
2			PdNPs@MIL-101	81
			PdNPs/PAs@MIL-101	100
3			PdNPs@MIL-101	71
			PdNPs/PAs@MIL-101	69
4			PdNPs@MIL-101	69
			PdNPs/PAs@MIL-101	82
5			PdNPs@MIL-101	25
			PdNPs/PAs@MIL-101	100
6			PdNPs@MIL-101	31
			PdNPs/PAs@MIL-101	67

ity of the former (entry 4). In the case of *trans*-4-octene (an inner alkene with low reactivity), a higher reaction yield was obtained with the PdNPs/PAs@MIL-101 catalyst (entry 5). Weaker interaction with PA molecules occurred due to the larger steric hindrance near the carbon–carbon double bond of the substrate, which might have prevented strong trapping by PAs and induced facile transfer on PdNPs for hydrogenation. Similarly, the reaction enhancement owing to PA was also observed for the aromatic alkene as substrate (entry 6).

Conclusions

In this study, MOF composites incorporating PdNPs and PA were prepared following a co-generation strategy. The selection of $NaPH_2O_2$ as the reductant resulted in $Pd(OAc)_2$ accommodation inside the MOF pores, following reduction to PdNPs along with the generation of PAs through the oxidation of $NaPH_2O_2$. The fabricated PdNPs/PAs@MIL-101 catalyst exhibited higher reactivity towards hydrogenation compared to PdNPs@MIL-101, which demonstrated that PA molecules interacted with the alkene substrates to induce the hydrogenation reaction. Further investigation of the positive effect of PA on hydrogenation is required.

Conflicts of interest

The authors declare no competing financial interest.

Acknowledgements

This research was carried out with support from JSPS KAKENHI Grant Number 19K05661.

References

1 G. Vilé, D. Albani, M. Nachtegaal, Z. Chen, D. Dontsova, M. Antonietti, N. López and J. Pérez-Ramírez, *Angew. Chem., Int. Ed.*, 2015, **54**, 11265.
2 L. Liu and A. Corma, *Chem. Rev.*, 2018, **118**, 4981.
3 R. M. Crooks, M. Zhao, L. Sun, V. Chechik and L. K. Yeung, *Acc. Chem. Res.*, 2001, **34**, 181.
4 L. Chen, H. Chen, R. Luque and Y. Li, *Chem. Sci.*, 2014, **5**, 3708.
5 H. Li, Z. Zhu, F. Zhang, S. Xie, H. Li, P. Li and X. Zhou, *ACS Catal.*, 2011, **1**, 1604.
6 M. Meilikhov, K. Yusenko, D. Esken, S. Turner, G. Van Tendeloo and R. A. Fischer, *Eur. J. Inorg. Chem.*, 2010, 3701.
7 J. Yu, C. Mu, B. Yan, X. Qin, C. Shen, H. Xue and H. Pang, *Mater. Horiz.*, 2017, **4**, 557.
8 O. M. Yaghi, M. O'Keeffe, N. W. Ockwig, H. K. Chae, M. Eddaoudi and J. Kim, *Nature*, 2003, **423**, 705.
9 S. Kitagawa, R. Kitaura and S. Noro, *Angew. Chem., Int. Ed.*, 2004, **43**, 2334.
10 G. Ferey, *Chem. Soc. Rev.*, 2008, **37**, 191.
11 H.-C. Zhou and S. Kitagawa, *Chem. Soc. Rev.*, 2014, **43**, 5415.
12 N. Wei, M.-Y. Zhang, X.-N. Zhang, G.-M. Li, X.-D. Zhang and Z.-B. Han, *Cryst. Growth Des.*, 2014, **14**, 3002.
13 L. Liu, X.-N. Zhang, Z.-B. Han, M.-L. Gao, X.-M. Cao and S.-M. Wang, *J. Mater. Chem. A*, 2015, **3**, 14157–14164.
14 M.-L. Gao, W.-J. Wang, L. Liu, Z.-B. Han, N. Wei, X.-M. Cao and D.-Q. Yuan, *Inorg. Chem.*, 2017, **56**, 511–517.
15 A. R. Millward and O. M. Yaghi, *J. Am. Chem. Soc.*, 2005, **127**, 17998.
16 J.-R. Li, Y. Ma, M. C. McCarthy, J. Sculley, J. Yu, H.-K. Jeong, P. B. Balbuena and H.-C. Zhou, *Coord. Chem. Rev.*, 2011, **255**, 1791.
17 J. L. C. Rowsell and O. M. Yaghi, *J. Am. Chem. Soc.*, 2006, **128**, 1304.
18 J.-R. Li, R. J. Kuppler and H.-C. Zhou, *Chem. Soc. Rev.*, 2009, **38**, 1477.
19 T. Uemura, N. Yanai and S. Kitagawa, *Chem. Soc. Rev.*, 2009, **38**, 1228.
20 J. Song, Z. Luo, D. K. Britt, H. Furukawa, O. M. Yaghi, K. I. Hardcastle and C. L. Hill, *J. Am. Chem. Soc.*, 2011, **133**, 16839.
21 R. W. Larsen, L. Wojtas, J. Perman, R. L. Musselman, M. J. Zaworotko and C. M. Vetromile, *J. Am. Chem. Soc.*, 2011, **133**, 10356.
22 D. T. Genna, A. G. Wong-Foy, A. J. Matzger and M. S. Sanford, *J. Am. Chem. Soc.*, 2013, **135**, 10586.
23 A. Grigoropoulos, G. F. S. Whitehead, N. Perret, A. P. Katsoulidis, F. M. Chadwick, R. P. Davies, A. Haynes, L. Brammer, A. S. Weller, J. Xiao and M. J. Rosseinsky, *Chem. Sci.*, 2016, **7**, 2037.
24 H.-L. Jiang and Q. Xu, *Chem. Commun.*, 2011, **47**, 3351.
25 C. Rosler and R. A. Fischer, *CrystEngComm*, 2015, **17**, 199.
26 H. Kobayashi, Y. Mitsuka and H. Kitagawa, *Inorg. Chem.*, 2016, **55**, 7301.
27 Q.-L. Zhu and Q. Xu, *Chem*, 2016, **1**, 220.
28 S. Y. Fong, N. M. Sánchez and A. de Klerk, *Energy Fuels*, 2019, **33**, 11677.
29 L. Peng, S. Yang, S. Jawahery, S. M. Moosavi, A. J. Huckaba, M. Asgari, E. Oveisi, M. K. Nazeeruddin, B. Smit and W. L. Queen, *J. Am. Chem. Soc.*, 2019, **141**, 12397.
30 V. V. Karve, D. T. Sun, O. Trukhina, S. Yang, E. Oveisi, J. Luterbacher and W. L. Queen, *Green Chem.*, 2020, **22**, 368.
31 G. Férey, C. Mellot-Draznieks, C. Serre, F. Millange, J. Dutour, S. Surblé and I. Margiolaki, *Science*, 2005, **309**, 2040.
32 T. Zhao, F. Jeremias, I. Boldog, B. Nguyen, S. K. Henninger and C. Janiak, *Dalton Trans.*, 2015, **44**, 16791.
33 A. Henschel, K. Gedrich, R. Kraehnert and S. Kaskel, *Chem. Commun.*, 2008, 4192–4194.
34 Y. Takashima, Y. Sato, N. Kubo, T. Tsuruoka and K. Akamatsu, *Chem. Lett.*, 2021, **50**, 244.

